Partial-wave analysis of the $K^+\pi^+K^-$ system seen in the reaction $\pi^+p \to K^+\pi^+K^-p$ at 11.46 GeV/c

I. D. Leedom, R. J. De Bonte, J. A. Gaidos, R. L. McIlwain, D. H. Miller, A. R. Moser,*
T. R. Palfrey, and D. J. Smith
Purdue University, West Lafayette, Indiana 47907

A. W. Key and M. Wong
University of Toronto, Toronto, Ontario, Canada M5S 1A7
(Received 2 November 1982)

We present results of a hybrid-bubble-chamber experiment examining the reaction $\pi^+p \to \pi^+pK^+K^-$ at an incident momentum of 11.46 GeV/c. The total cross section for this channel is determined to be $87.2 \pm 6.4\ \mu$b. A partial-wave analysis of the $K^+\pi^+K^-$ system reveals no unambiguous evidence of resonant activity, although mass enhancements are noted in the $J^P=0^-$ $\bar{\kappa}K^+$ (S wave), $J^P=2^-$ $f\pi$ (S wave), and $J^P=2^-$, $\bar{K}^{*0}(892)K^+$ (P wave). This is the first published report of the relative phases of the waves seen in this reaction. We comment on the influence this channel may have on A_1 and A_3 production.

I. INTRODUCTION

We present results from a partial-wave analysis of inelastic pion diffractive dissociation in the reaction $\pi^+p \to K^+\pi^+K^-p$ at an incident pion momentum of 11.46 GeV/c. This is the first such study to our knowledge in which the relative production phases of the contributing waves have been measured. Our results are obtained from four times as many events as any previous bubble-chamber analysis.[1] They are derived from experiment BC-61 which utilized the SLAC hybrid-bubble-chamber facility (SHF) with an unseparated π^+ beam. The large geometrical acceptance of the system coupled with the 4π solid-angle coverage of the bubble chamber obviates the need for the large systematic corrections (and their attendant errors) associated with high-statistics counter experiments.

A great deal of attention has been focused on the $\pi\pi\pi$ final state and the references we quote are by no means exhaustive.[2-6] This interest stems in part from the conflicting reports of resonant activity in the three-pion system connected with the A_1 and A_3 states. In the case of the A_1, there has been theoretical speculation[7] that the opening of the $\bar{K}^{*0}K^+$ threshold could affect the $\rho\pi$ system in the same fashion that the $K\bar{K}$ threshold influences $\pi\pi$ scattering. No study has yet possessed sufficient statistical significance to resolve this or to determine whether there are any resonant $K^+\pi^+K^-$ states. With this paper we attempt to answer these questions.

The rest of this paper is divided into five sections. In the first is discussed the layout and operation of the SHF. The second section concerns the reduction and the selection of the data sample. The fitting procedure is described in the third section, while the results and conclusions are found in the fourth and fifth sections, respectively.

EXPERIMENTAL ARRANGEMENT

The SHF, shown in Fig. 1, has the beam-defining elements: (1) scintillator paddle $S1$, (2) first proportional wire chamber PWC 1, (3) the freon-filled beam Cherenkov counter CB, (4) the four-segment

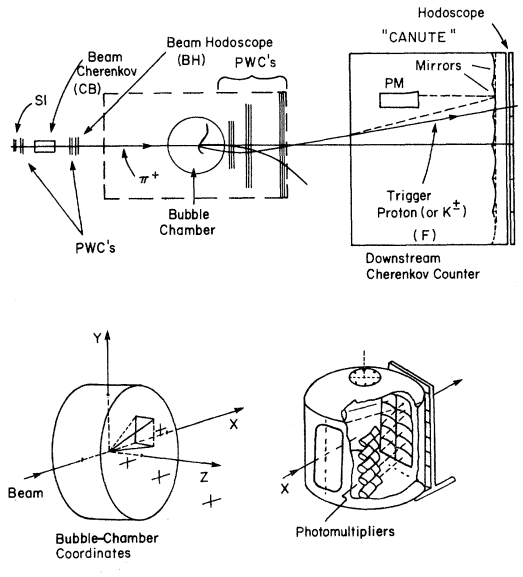

FIG. 1. Diagram of the SLAC hybrid-bubble-chamber facility.

beam hodoscope BH, and (5) PWC 2. The bubble chamber is the 40-in. (100-cm) rapid cycling-chamber utilizing a liquid hydrogen target in a 26-kG magnetic field. Downstream particle trajectories were tracked by three PWC stations (α, β, and γ), a ten-element freon Cherenkov detector C with a threshold at a γ of 18, and a segmented hodoscope whose elements matched those of the Cherenkov counter. The bubble chamber was run at a rate of 10—12 Hz, with an average of six particles per beam spill. The upstream PWC stations consisted of two perpendicular wire planes (y and z) while the downstream configurations included a third (u) plane at an angle of 37° with respect to the y plane. The wire-chamber resolution was 1.1 mm. Further details may be found in the literature.[8]

The system employed two separate triggers to screen candidate events: these will be referred to as the hardware and software triggers. The hardware trigger consisted of logic-level pulses from $S1$, CB, and BH to identify a good beam pion. With the beam Cherenkov CB operated in the threshold mode, its analog pulse was split, with one part discriminated to form the logical pulse and the other digitized for use in the software trigger. The purpose of the downstream apparatus was to eliminate events with fast pions. As such, it both removed the fast pion-producing reactions and served as an event veto. A fast pion was defined as one which had a momentum greater than 4.2 GeV/c. The light intensity produced in all cells in the downstream Cherenkov detector C was denoted as CSUM. Signals from the individual elements of C (again split so that they could be digitized) were summed and required to be less than CSUM. This was coupled with the requirement that there be at least one hit in the hodoscope, H. The hardware trigger is thus written as

$$(S1\cdot\mathrm{CB}\cdot\mathrm{BH})\cdot(\overline{\mathrm{CSUM}}\cdot H)\ .$$

The nominal hardware trigger gate was 10 nsec and on the average, there was one hardware trigger for every 17 beam pions.

Upon receipt of a hardware trigger the electronics were gated off for $\sim$150 nsec to allow the PWC hits and digitized Cherenkov signals to be read into an on-line DGC NOVA minicomputer. After this time the system was again opened, although no more than two hardware triggers were allowed in any one beam spill. This latter constraint was imposed by the processing time of the software algorithm ($\sim$1—2 msec) and the optimum time for bubble growth. The software trigger employed the PWC information along with the known magnetic-field map to follow the outgoing tracks downstream and to connect these with the upstream wire-chamber tracks to determine that the interaction vertex did indeed lie within the fiducial volume. The outgoing track's momentum was computed and required to be greater than 4.5 GeV/c. The amount of light to be expected from a kaon or proton of this momentum was compared to the digitized signals from C and the two required to be comparable. In test runs using Monte Carlo events, the software trigger was shown to reject efficiently events with fast pions and select events with kaons or protons above 4.5 GeV/c. When the software algorithm was satisfied, an exposure was taken. During the running of the experiment, approximately one frame was exposed for every 160 beam particles.

THE DATA SAMPLE

Data reduction took place at Purdue University and the University of Toronto. Only four-prong topologies with no visible vees or pairs were scanned. Events satisfying these constraints were kept only if the event vertex lay within $\pm$10 wire numbers of the wire associated with the triggering beam track. Track digitization at both institutions employed POLLY semiautomatic measuring machines and kinematical track reconstruction was accomplished with the TVGP-SQUAW series with one important addition: a program, HYBRID, was used to extend the beam and outgoing tracks to the PWC stations where they were linked with the wire hits in order to refine the measured quantities. The effect of this track linking is shown in Fig. 2, where the errors of the fitted momenta for kaons before and after "hybridization" have been plotted.

An important consideration for any triggered experiment is the acceptance of the system. The geometrical acceptance of the system was examined in the following fashion: (1) Each real event was moved in turn to one of 12 positions in the bubble chamber covering the spatial range of the beam. (2) At each position these new events were rotated about the beam axis to six different azimuthal angles. (3) For each new position and angle, the tracks were projected downstream and subjected to the same requirements as the software trigger. The average acceptance so determined was 80$\pm$4%. Of the 1.2×10^6 pictures scanned, 10 688 gave at least one four-constraint fit to the reaction of interest and had an acceptance for that fit of 20% or greater.

For cross-section calculations, fitted event ambiguities were resolved by weighting each fit by its confidence level (as calculated by SQUAW) divided by the sum of all confidence levels for the event. Only fits with a confidence level greater than 0.05% were considered. Events which remained after the fiducial volume cut were corrected for systematic

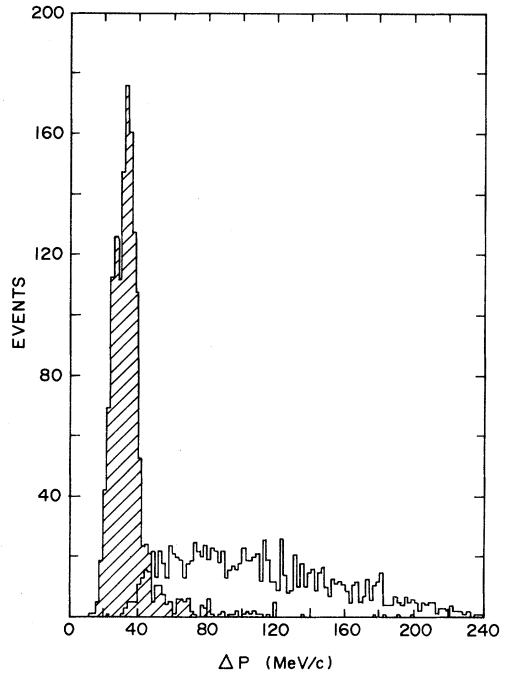

FIG. 2. Error in the fitted momentum for fast leaving kaons. The unshaded and shaded histograms correspond to the event sample before and after "hydridization."

losses. The correction factors and errors are given in Table I. A brief discussion of each follows.

Downstream interactions. Potential triggering tracks may be removed through inelastic collisions with the downstream apparatus. The loss has been computed by using the known cross section[9] for kaons and protons of momenta 4—10 GeV/c.

δ *rays.* Produced primarily in the wall of the downstream Cherenkov counter, energetic electrons ($E > 15$ MeV) may produce enough light to veto a trigger. The correction was computed using the known distribution of incident particles on the face of the Cherenkov detector.[10]

Kaon decays. The decay in flight of a fast kaon both removes a possible triggering track and produces an energetic pion or muon. The three largest decay modes ($K^{\pm}\to\mu^{\pm}\nu$; $\pi^{\pm}\pi^{0}$, $\pi^{\pm}\pi^{\pm}\pi^{\pm}$) were considered. The loss rate for a single kaon was 3.1% and 5.3% for two. The final correction factor represents an average over the entire data sample.[11]

Untriggered events. Because of the range of wire numbers used in event scanning, it was possible for events to be selected for measuring when they had not in fact triggered the system. The effect is to add events to the sample and as a result the correction factor is less than one.

Throughput. This factor represents the correction for losses in scanning, measuring, TVGP-SQUAW processing, and the minimum-confidence-level cut. It was determined by comparison of the four-constraint fits found on 48 film rolls measured by both Purdue and Toronto.

Acceptance. This figure accounts for the good events which did not trigger because of the geometry of the system or because of wire-chamber inefficiencies.

"Invisible" events. The acceptance correction does not account for that class of events which, while representing the proper final state, could never trigger the system. This occurs in general because such events include a fast pion. The value presented was calculated using similar events from an untriggered bubble-chamber experiment at an incident pion momentum of 13.2 GeV/c. The details of this experiment have been previously reported.[12] The trigger was simulated by longitudinal momentum (i.e., that component of the momentum along the beam axis) cuts on the outgoing kaons and pions. The demands of this experiment, to wit that $p_K \geq 4.5$ GeV/c and $p_\pi \geq 4.2$ GeV/c, were scaled by the ratio of the two-beam momenta to account for the increase in available phase space. The error includes the statistical error and the error in the beam momenta. The value quoted is for the entire reaction. The parenthetical quantity is for those events used in the partial wave analysis.

The beam-flux corrections can be divided into two types, rate dependent and rate independent. The rate-independent corrections are from an 8% μ contamination and the upstream beam interactions. The rate-dependent corrections were assessed on a roll-by-roll basis using the average number of particles per beam spill. All these are shown in Table II. The first three rate-dependent factors are calculated using the experimentally determined dead times and

TABLE I. Corrections to the total number of events.

Cause	Correction factor
Downstream collisions	$C_1 = 1.06 \pm 0.03$
Kaon decays	$C_2 = 1.034 \pm 0.010$
δ rays	$C_3 = 1.01 \pm 0.005$
Acceptance	$C_4 = 1.25 \pm 0.05$
Throughput[a]	$C_T = 1.54 \pm 0.12$
	$C_P = 1.45 \pm 0.11$
	$C_B = 1.12 \pm 0.04$
Untriggered events	$C_5 = 0.99 \pm 0.01$
Events invisible to the trigger	$C_6 = 1.30 \pm 0.05$ (1.27±0.06)

[a]The value of the throughput correction depended on which institution measured the film. The meaning of the subscripts is as follows: T=Toronto; P=Purdue; B=both institutions. The average throughput was 1.48±0.11.

TABLE II. Beam losses.

Name	Correction factor	Loss (%)
Fast trigger	0.92	8.9±1[a]
ADC pileup	0.95	4.9±1[a]
Upstream PWC	0.97	3.0±2[a] (14 ±5)[b]
More than two particles in upstream PWC	0.96	3.6±0.6[a]
More than 12 particles in a beam spill	0.99	0.8±0.3[a]
Muon contamination	0.92	8.0±2
Upstream interactions	0.94	6.1±0.7

[a]Losses computed for six particles per spill (3.75 MHz).
[b]The first number refers to the loss with two upstream PWC's in use, a configuration in which most of the data was taken. The second value applies to the loss with only one PWC in operation.

a nominal beam spill of six particles per pulse. These losses are the following.

Fast trigger. This is an effective dead time (24 nsec) to account for the time in which the electronics was gated off for the PWC's to be read out.

ADC pileup. A good trigger could be vetoed by the downstream Cherenkov counter if a beam track was within the gate of the analog-to-digital converter (ADC).

Upstream PWC inefficiency. Because the beam was spread across a small area of the wire chambers, it was possible for a track to be lost due to the individual wire deadtime.

More than two beam tracks in the upstream PWC. In order to reduce processing time in the software algorithm, any event with more than two beam tracks in the upstream wire chambers was vetoed.

More than 12 particles in the beam spill. Beam spills of this nature were vetoed in the hardware. The reason was to render the exposures easy to scan and measure. The loss is computed assuming a Poisson distribution for the number of beam particles. The final pion flux was $(1.18\times10^8)\pm4.8\%$ particles corresponding to a sensitivity of 260 ± 10 events/μb. The total number of weighted events after correction for the throughput, roll, and fiducial volume selections was 12731. The total cross section is thus calculated to be 87.2 ± 9.3 μb. In Fig. 3, this result is shown along with those of other experiments at different beam momenta.

We turn our attention to the consideration of the events used in the partial-wave analysis. The demand of peripherality is made by requiring that $-t'$ from incoming to outgoing proton be less than 0.5 (GeV/c)^2. To eliminate contamination from resonance production, the conditions that $M(\pi^+p)\geq1.4$ GeV/c^2 and $M(K^-p)\geq1.55$ GeV/c^2 were imposed. In this way we eliminate the majority of events involving $\Delta^{++}(1232)$ and $\Lambda(1520)$ production. The final sample consists of 2033 unique four-constraint fits to the reaction of interest, all of which lie in the $K^+\pi^+K^-$ mass region from 1.4 to 2.4 GeV/c. The cross section for this subset is 19.4 ± 2.1 μb. This result is shown along with those for the same reaction at lower and higher beam momenta[13] in Table III. The differential cross sections have been parametrized by the form $d\sigma/dt'\propto e^{bt'}$ and the slope parameters determined in 200-MeV intervals. The results are displayed in Table IV along with those of a bare bubble-chamber experiment[1] at a beam momentum of 16 GeV/c. As can be seen, there is no strong dependence of the slope on the incident pion momentum. Comparison of the total and differential cross sections reveals only a slow change with energy as is expected for a diffractive production mechanism.

The acceptances as a function of the mass of the $K^+\pi^+K^-$, K^+K^-, and π^+K^- systems along with those mass spectra are shown in Figs. 4—6. The errors on the acceptance reflect the statistical uncertainty in each mass interval. The acceptance is flat within errors in all cases but does show a small increase at low K^+K^- mass. The increase is a reflection of the possibility that both kaons can trigger the system. The net effect is negligible. Were there an acceptance related effect, it is more likely that it would be manifested in the angular distributions.[8] The angular variables chosen are the polar and azimuthal angles of the K^- in the three-meson rest frame, θ and ϕ, and the angle between the decay and production planes, γ. The distributions for these angles are shown in Figs. 7—12, where the first three plots are for the mass region 1.4—2.0 GeV/c^2 and the second three for 2.0—2.4 GeV/c^2. There is no appreciable effect for the lower mass sample, but the θ and γ distributions in the high-mass group show a pronounced variation. Further investigation has shown this to be entirely due to a small number of events (5% of the data in this mass range) with acceptances less than 40%. The effect on the fits has been examined by generating events weighted by the inverse of the acceptance. Within errors, the results

TABLE III. Total cross section for inelastic diffractive dissociation in the reaction $\pi^+p\rightarrow\pi^+pK^+K^-$.

Beam momentum (GeV/c)	σ (μb)	Reference
8.00	18±5	Bosseti *et al.* (Ref. 13)
11.46	19.4±2.1	This experiment
16.00	25^{+6}_{-2}	Bosseti *et al.* (Ref. 13)

TABLE IV. Exponent of the differential cross section as a function of $\pi^+K^+K^-$ mass in GeV/c^2.

	Beam momentum (GeV/c)	Mass regions (GeV/c^2) 1.4–1.6	1.6–1.8	1.8–2.0	2.0–2.2	2.2–2.4
$-t' \leq 0.5$ (GeV/c)^2	11.46	5.1±0.5 1.4–1.8	6.5±0.4	6.3±0.5 1.8–2.2	3.6±0.5	5.0±0.6
$-t' \leq 0.8$ (GeV/c)^2	16.00	5.8±0.4		5.1±0.5		

were the same. We conclude that no specific acceptance-related correction is required.

THE FITTING PROCEDURE

The fitting was performed using the Illinois partial-wave-analysis program.[1,2,14] The states used are characterized by the quantum numbers J, P, L, M, and η. The decay of this state is seen as a two-step process which is illustrated in Fig. 13. The first decay is into an isobar and a bachelor meson with relative orbital angular momentum L. Then the isobar decays into two spinless mesons. The isobars used in the fitting are listed in Table V along with their masses and widths. We choose to represent the S-wave resonances by relativistic Breit-Wigner formulas rather than the corresponding phase shifts. In the case of the S^*, it may be argued that the evidence favors a polar position below $K\bar{K}$ threshold, but all fits showed a negligible ($<5\%$ of the data in any mass interval) contribution from this state and such a choice may therefore be justified *a posteriori*. The κ is a knottier problem; neither the $K\pi$ phase shifts nor the Breit-Wigner formulation seem sufficient to explain the observed behavior. The fits are, however, insensitive to large changes in the mass and width of the κ and we are thus led to use the parametrization of Otter *et al.*[1]

Of the states attempted, only those with $\eta = +1$, corresponding to natural-parity exchange, and $M=0$ were found to contribute. As a result the states employed are referred to by the nomenclature J^PL, $\eta = +1$ and $M=0$ being assumed.

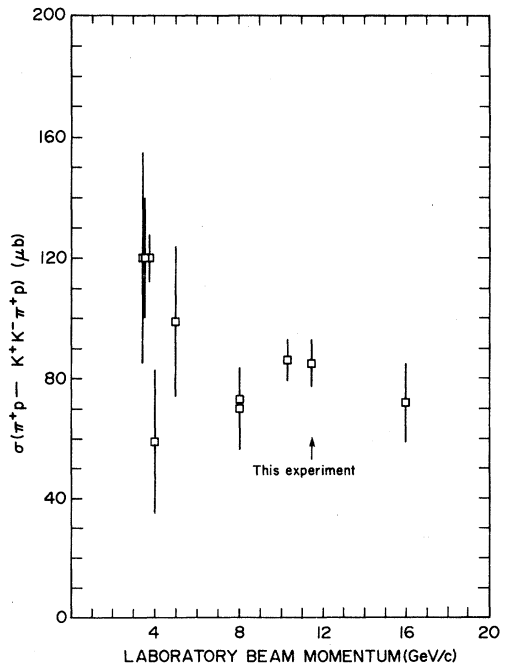

FIG. 3. Cross section for the reaction $\pi^+p \to K^+K^-\pi^+p$ as a function of beam momentum.

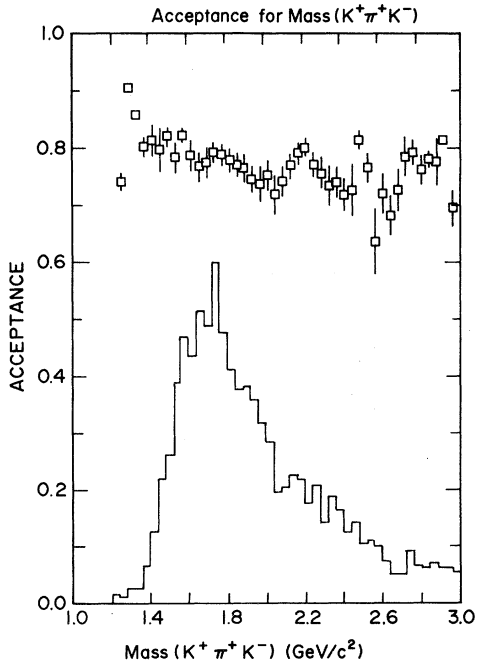

FIG. 4. Acceptance as a function of the invariant mass of the $K^+\pi^+K^-$ system subject to $M(\pi^+p) > 1.4$ GeV/c^2, $M(K^-p) > 1.55$ GeV/c, and $-t' \leq 0.5$ (GeV/c)^2. In this and subsequent figures, the actual distribution of data is indicated by a histogram.

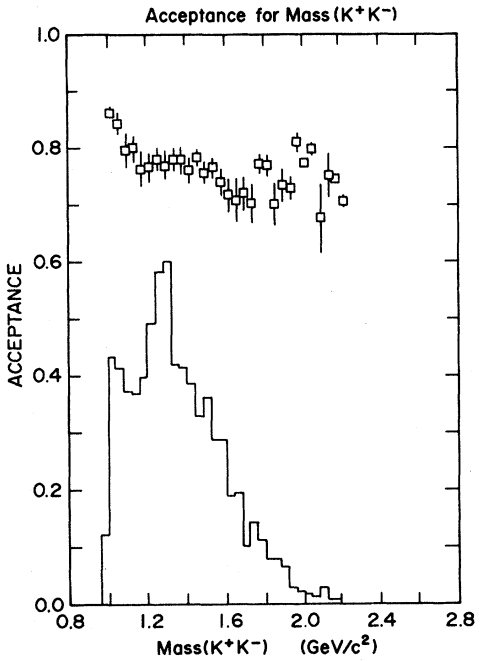

FIG. 5. The acceptance as a function of the invariant mass of the K^+K^- system for the partial-wave-analysis data sample.

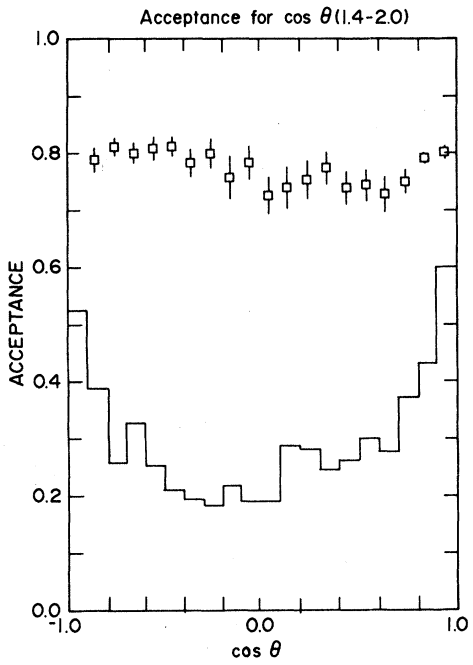

FIG. 7. The acceptance as a function of the polar angle, θ, in the t-channel frame for the three-meson mass range 1.4—2.0 GeV/c^2.

The stability of the fits was examined in two ways. First the starting values of the fitting parameters were varied over a region much larger than the associated errors of the parameters. Within reason-

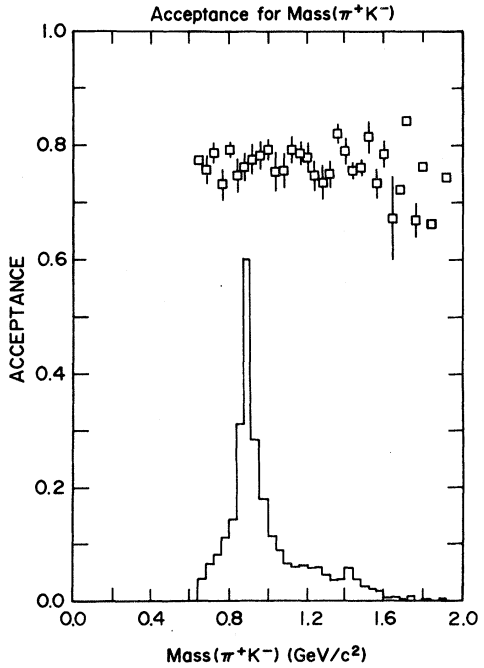

FIG. 6. The acceptance as a function of the invariant mass of the π^+K^- system for the partial-wave-analysis data sample.

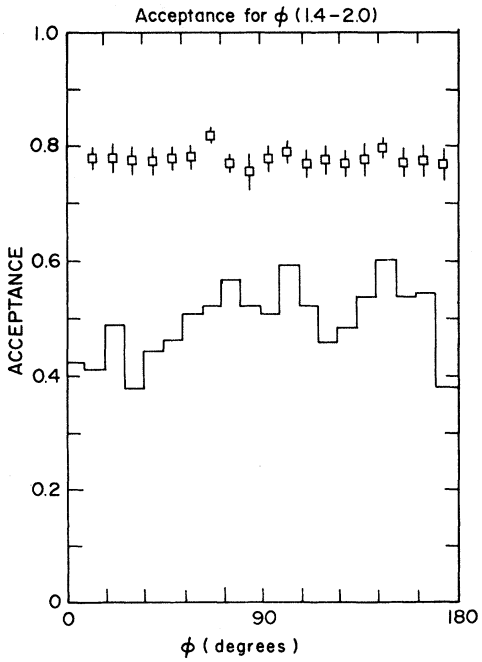

FIG. 8. The acceptance as a function of the azimuthal angle, ϕ, in the t-channel frame for the three-meson mass range 1.4—2.0 GeV/c^2.

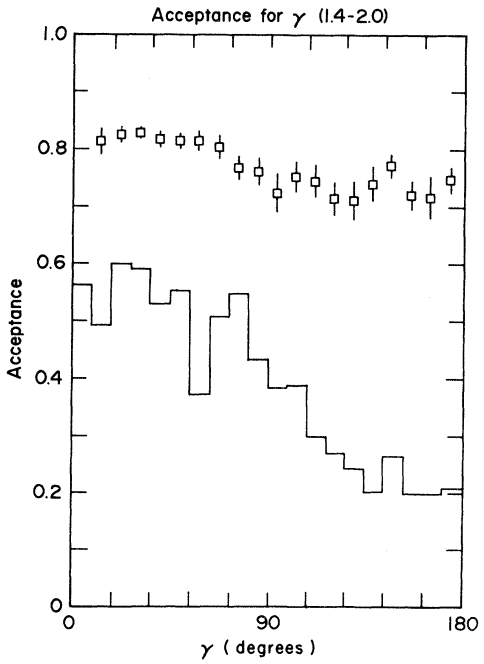

FIG. 9. The acceptance as a function of the Euler angle γ for the three-meson mass range 1.4—2.0 GeV/c^2.

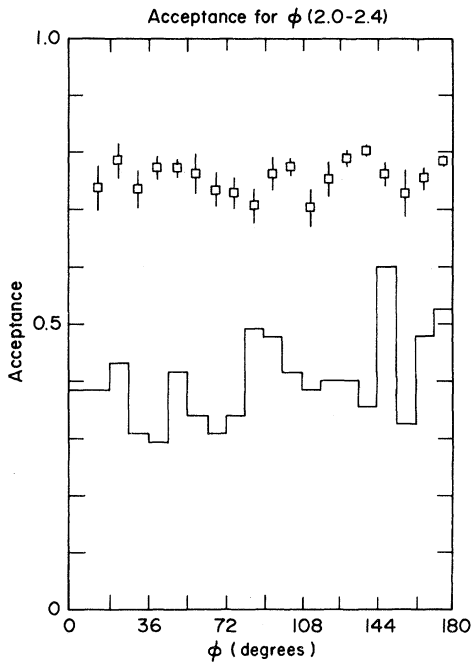

FIG. 11. The acceptance as a function of ϕ for the mass range 2.0—2.4 GeV/c^2.

able limits, the results were always the same. Second, the logarithmic likelihood function was shown to be quadratic in the parameter errors subject to the constraint that the diagonal elements of the density matrix be greater than or equal to zero. Finally, as a check on the quality of the results, events were generated by Monte Carlo simulation using the fitted parameters. The effect of the trigger

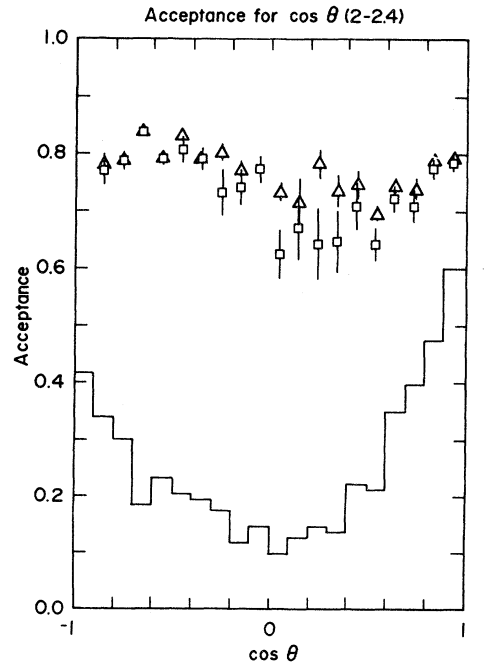

FIG. 10. The acceptance as a function of θ for the mass interval 2.0—2.4 GeV/c^2. □, acceptance ≥ 0.2; Δ < acceptance ≥ 0.4 (see text).

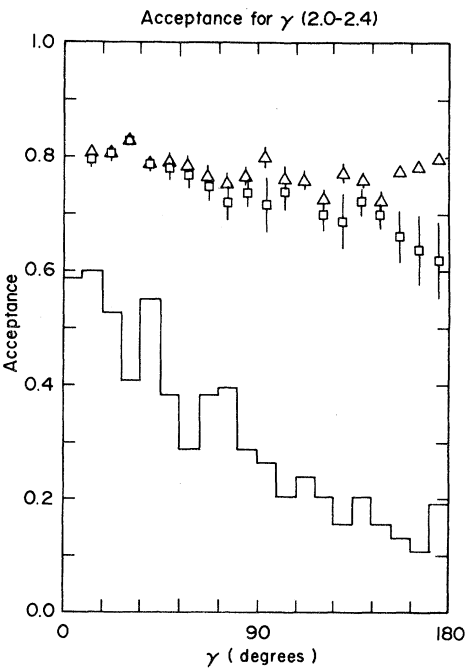

FIG. 12. The acceptance as a function of γ for the mass interval 2.0—2.4 GeV/c^2. □, acceptance ≥ 0.2; Δ, acceptance ≥ 0.4 (see text).

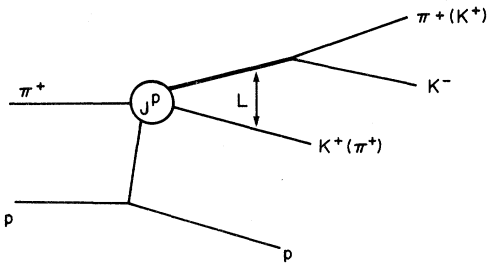

FIG. 13. Pictorial representation of the production of the state of spin-parity J^P and its two-step decay.

was imposed by demanding that the laboratory longitudinal momentum of one of the kaons be greater than 4.5 GeV/c and that the pion's longitudinal momentum be less than 4.2 GeV/c. Comparisons of the experimental and Monte Carlo data for the angular distributions are shown in Figs. 14–16. In all cases the fits to the experimental data were acceptable.

The procedure was to introduce only low partial waves at first and to add higher spins only if they increased the likelihood, gave a contribution which was greater than zero, and appeared in more than one mass interval. The last condition was necessitated to eliminate "one bin" effects. The "flat" state which represents a decay into three uncorrelated mesons and which does not interfere with any other amplitude was found to make no significant contribution and was dropped. No states were required with spins greater than 2.

RESULTS

The intensities of the contributing waves over the $K^+\pi^+K^-$ mass range 1.4–2.4 GeV/c^2 are listed in Table VI and displayed in Fig. 17. It is apparent that S waves dominate. The only major exceptions are the 1^+P ($\bar{\kappa}K^+$) and 2^-P ($\bar{K}^{*0}(892)K^+$) states. As has been previously noted,[1] the κ plays a much more important role in the $K^+\pi^+K^-$ final state than the ϵ does in the corresponding $\pi^+\pi^+\pi^-$ case. The only K^+K^- isobar which contributes is the $f^0(1271)$ which appears only in the 2^-S wave. Our approach is to discuss each spin-parity state in turn.

$J^P = 0^-$

The 0^- state is due almost entirely to S-wave $\bar{\kappa}K^+$ production. No evidence was found for significant $S^*\pi^+$ production. On the basis of $\frac{1}{4}$ the number of events present in this analysis, Otter *et al.*[1] concluded that their analysis could not differentiate between the two possibilities. Our work shows that the 0^-S wave is entirely due to $\bar{\kappa}K^+$. The mass spectrum is flat except for an enhancement centered at 1.75 GeV/c^2. Recently, Bellini *et al.*[15] have cited evidence from a three-pion final state for a 0^-S resonance in this region which was tentatively associated with a radial excitation of the pion. Examination of the phase shifts (Fig. 18) shows a mixed result. The 1^+P phase differences are essentially flat over the entire mass region. The 1^+S phase shifts, on the other hand, drop some 30° from their threshold values, advance 60°, and then drop to form a cusp in the 1.8–1.9 GeV/c^2 mass interval. Neither piece of evidence argues for a resonance interpretation. It may be, however, that the cusp in the 0^-S-1^+S phase difference is due to the opening of some other channel. Toet *et al.*[16] found a relatively large cross section (15 ± 10 μb) for K^+K^- and three or more pions in an experiment using a π^+ beam of momentum 5 GeV/c. This may account for the 1^+S wave phase phenomenon, but the 1^+P wave behavior continues to militate against a resonant 0^-S wave.

The other contribution to the 0^- state is from 0^-P ($\bar{K}^{*0}(892)K^+$). It is small and appears only in the first three mass intervals. With such limited statistics, we must restrict ourselves to merely noting that it appears.

$J^P = 1^+$

The 1^+ partial wave is the largest in the sample, comprising over 40% of the data. Two waves contribute to this total, 1^+S ($\bar{K}^{*0}(892)K^+$) and 1^+P ($\bar{\kappa}K^+$). The proportion of P wave to S wave is three times larger in the $K^+\pi^+K^-$ case than in the corresponding $\pi^+\pi^+\pi^-$ final state. The general features of the S and P waves are apparent from Figure 17. The S wave rises rapidly from threshold into a large

TABLE V. Isobars used in partial-wave analysis.

Name	J^P	S	Mass (GeV/c^2)	Width (GeV/c^2)
κ	0^+	-1	1.245	0.48
$K^*(890)$	1^-	-1	0.892	0.052
$K^*(1432)$	2^+	-1	1.432	0.100
S^*	0^+	0	0.995	0.040
f^0	2^+	0	1.271	1.800

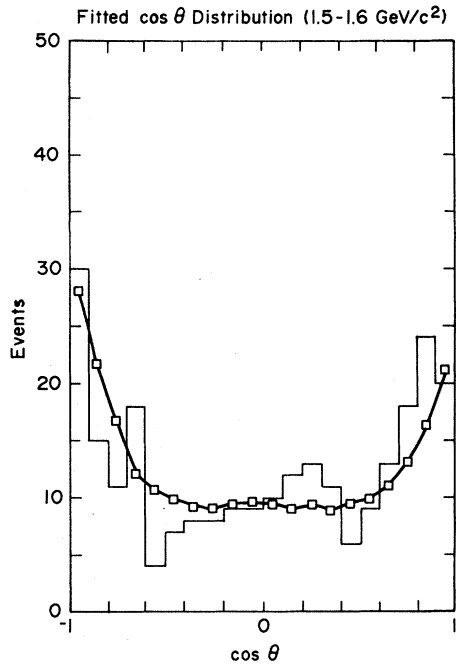

FIG. 14. Fitted and experimental $\cos\theta$ distributions in the $K^+\pi^+K^-$ mass interval 1.5—1.6 GeV/c^2.

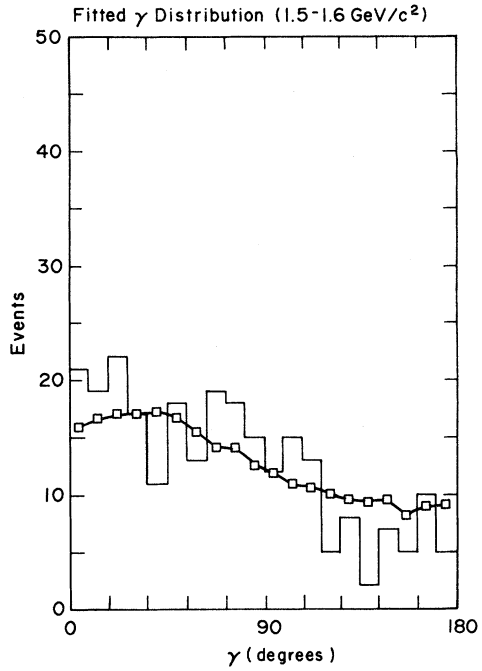

FIG. 16. Fitted and experimental γ distribution in the $K^+\pi^+K^-$ mass interval 1.5—1.6 GeV/c^2.

bump roughly centered at 1.7 GeV/c^2, then declines. The P-wave intensity shows more of a plateau structure, not rising until 1.6 GeV/c^2 and remaining constant thereafter.

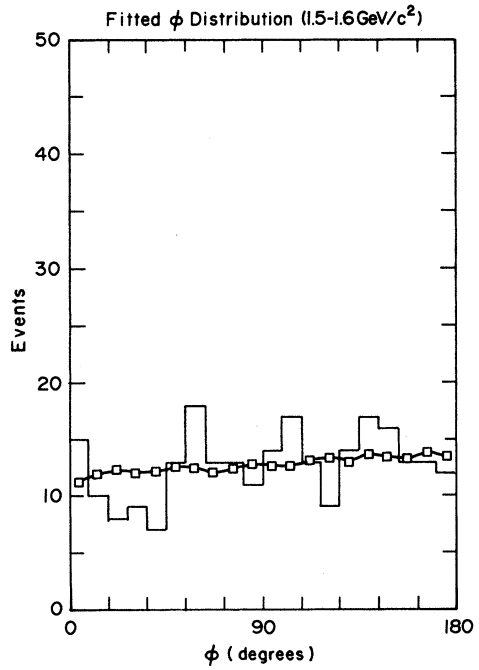

FIG. 15. Fitted and experimental ϕ distribution in the $K^+\pi^+K^-$ mass interval 1.5—1.6 GeV/c^2.

The phase behaviors of both waves are more complicated. The 1^+S ($\bar{K}^{*0}(892)K^+$) state has been of interest for some time.[7,17] In the three-pion system, the 1^+S $\rho\pi$ waves show an enhancement some 200 MeV above $\rho\pi$ threshold, which is traditionally associated with the A_1. There are conflicting reports[5,18] on the mass of this object. Statistically speaking, the analysis of the Amsterdam-CERN-Cracow-Munich-Oxford-Rutherford (ACCMOR) collaboration is generally accepted as the definitive work. They find evidence for a resonant A_1 with a mass of 1.28 GeV/c^2 and half-width of 0.28 GeV/c^2, a value higher than that seen in either diffractive or baryon-exchange reactions. These latter experiments find a lower value for the mass $\sim$1.1 GeV/c^2. The 1^+S phase differences are shown in Fig. 19 along with the corresponding ACCMOR three-pion data from Daum *et al.*[5] These latter phase shifts are for the three-pion mass region from 1.0—1.6 GeV/c^2 and thus correspond to roughly the same effective mass above threshold. The data are certainly similar, but for the 1^+S-0^-S data around 1.8 GeV/c^2, a difference to which we have already alluded. It would appear that the same production mechanism is at work. It is also apparent that the phase difference does not advance by the 90° which would indicate resonance production.

Returning to the question of the diffractive three-pion production, it has been noted that there also the 1^+S phase differences do not advance by

TABLE VI. Partial-wave intensities as a function of $K^+\pi^+K^-$ mass in GeV/c^2.

Wave $J^PLM\eta$	1.4–1.5	1.5–1.6	1.6–1.7	1.7–1.8	1.8–1.9	1.9–2.0	2.0–2.1	2.1–2.2	2.2–2.3	2.3–2.4	Total events
0^-S0+	75±14	87±19	88±22	160±24	114±21	79±17	80±16	74±17	54±16	73±15	884
0^-P0+	7± 5	25± 9	30±11								62
1^+S0+	41±13	110±19	125±18	134±22	77±22	69±17	48±10	27±10	34±11	48±11	713
1^+P0+	21± 8	26±14	64±17	50±14	46±15	58±16	53±12	50±15	11± 7		379
2^-S0+[a]		49±12	49±14	34±13							132
2^-P0+				45±13	91±18	50±12					186
2^-S0+[b]					8± 6	22±20	13± 7	23± 8	22± 8	3± 4	91
2^-D0+									36±11	20±11	56
Real events	126	255	308	346	259	218	156	138	119	110	2035
Total events	144	296	356	429[c]	337	279	193	173	157	144	2508
Parameters	11	13	13	13	13	13	11	11	13	11	

[a] $f^0\pi^+$.
[b] $K^*(1434)K^+$.
[c] Includes five $2^-S(f^0\pi^+)$-2^-P interference events.

90°, and this has been taken as evidence the 1^+S system is not resonant. Basdevant and Berger[7] have argued that this is due to the influence of the opening of the $\bar{K}^{*0}K^+$ threshold which might reasonably be expected to affect the $\rho\pi$ phase shifts in the same way that $K\bar{K}$ production influences the S wave in $\pi\pi$ scattering. We have examined this possibility by comparing the predictions of Ref. 7 for 1^+S ($\bar{K}^{*0}(892)K^+$) production between 1.4 and 1.8 GeV/c^2. The results are displayed in Fig. 20. In Fig. 20(a) is shown a fit to pure Deck production, while in Fig. 20(b) is displayed the fit using both Deck and direct production of a resonant A_1 with a mass of 1.3 GeV/c^2 and half-width of 400 MeV. The data obviously favor the first possibility. We conclude that 1^+S production is kinematical in nature. To summarize, neither the 1^+S nor the 1^+P waves show evidence of resonant activity.

$J^P=2^-$

The 2^- state derives contributions from the S waves ($f^0\pi^+$) and ($\bar{K}^{*0}(1434)K^+$), the P wave ($\bar{K}^{*0}(892)K^+$), and the D wave ($\bar{\kappa}K^+$). The latter state only contributes in the final two mass bins so that the paucity of data precludes any further analysis. The other three waves are more prominent and occupy different regions of the $K^+\pi^+K^-$ mass spectrum, and we discuss each in turn.

The 2^-S ($f^0\pi^+$) state appears shortly after threshold and persists through three mass intervals. No structure is immediately apparent. The phase

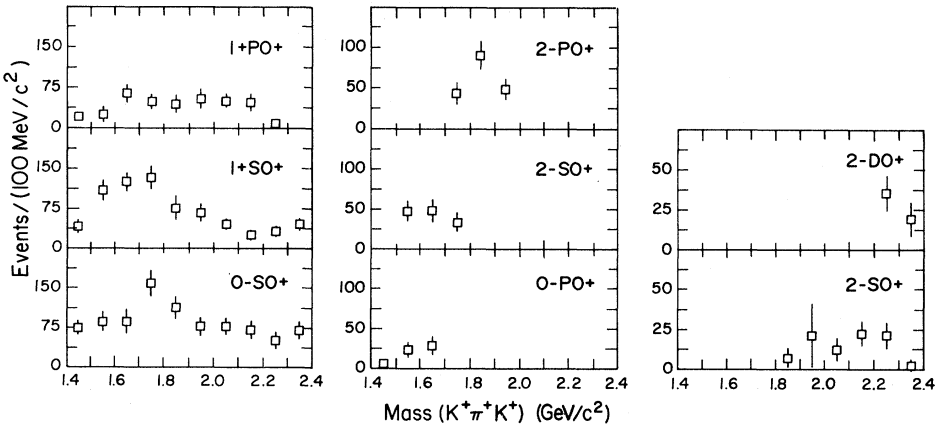

FIG. 17. The partial-wave intensities from 1.4–2.4 GeV/c^2.

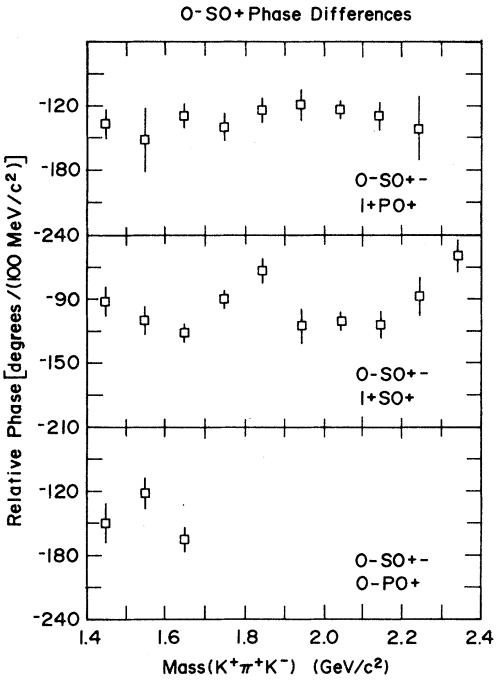

FIG. 18. The 0^-S phase differences with respect to the 0^-P, 1^+S, and 1^+P waves.

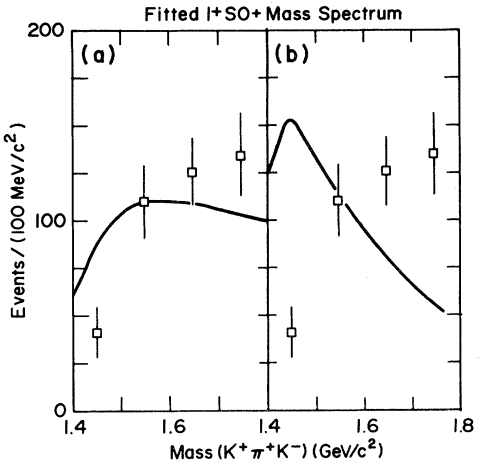

FIG. 20. (a) Comparison of 1^+S intensity with pure Deck-model production. (b) Comparison with both Deck-model and direct production of A_1 meson coupled to $\bar{K}^{*0}K^+$. Both taken from Ref. 7.

differences $2^-S - 0^-S$ and 1^+S both rise (Fig. 21), by 50° in the first instance and 30° in the second. The phase shift of the 0^-P wave also appears to increase though the data show considerable scatter. The small size of these phase changes and the lack of a definable mass peak would militate against a

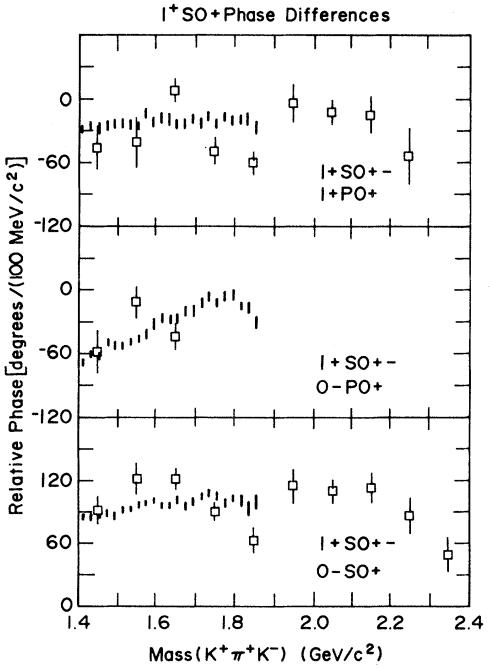

FIG. 19. The 1^+S phase differences with respect to the 0^-S, 0^-P, and 1^+P waves. □, this experiment; |, $\pi^+\pi^-\pi^-$ phase differences from Daum *et al.* (N. B. the three-pion phase differences have been moved so as to show the trend of the present data.)

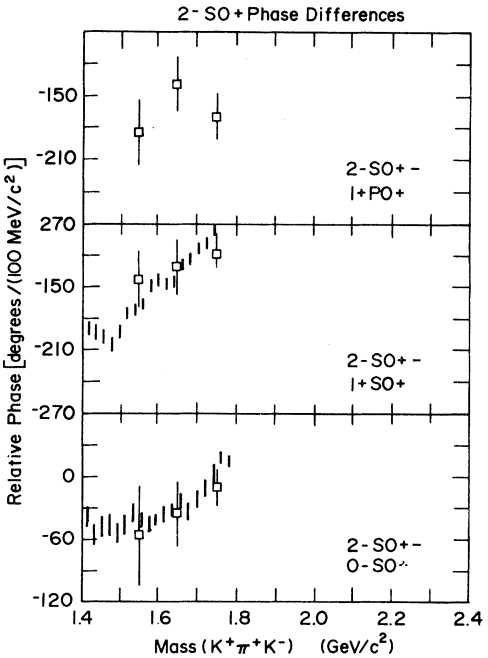

FIG. 21. The $2^-S\,f^+$ phase differences with respect to the 0^-S, 1^+S, and 1^+P waves. □, this experiment; |, $\pi^+\pi^-\pi^-$ phase differences from Daum *et al.* (Ref. 5). (N. B. the three-pion phase differences have been moved so as to show the trend of the present data.)

resonant interpretation were it not that these phase shifts show the same behavior as the three-pion data (again taken from Ref. 5), where the examination of a larger mass interval showed the resonant behavior of the A_3. In this instance both sets of data correspond to the same mass.

It is tempting to associate these events with the A_3; unfortunately, it is impossible to confirm or deny the resonant nature of our sample given the small number of events and the limited mass range. It is, however, possible to compare the production cross section of $f^0\pi^+ \to \pi^+\pi^-\pi^+$ and $f^0\pi^+ \to K^+\pi^+K^-$. There are 132 events attributed to the 2^-S $(f^0\pi^+)$ state in this experiment. Using an event correction factor of 2.63 and a sensitivity of 260 events/μb yields a cross section of 1.3 ± 0.1 μb. Thompson *et al.*[4] found a 2^-S $(f^0\pi^+)$ cross section into $\pi^+\pi^+\pi^-$ of 28 ± 5 μb at a beam momentum of 13.1 GeV/c. The branching ratio of f^0 to $K\bar{K}/\pi\pi$ is given by the Particle Data Group as 0.0339 ± 0.003, yielding an expected value of 1.0 ± 0.2 μb, in good agreement with the value found in this experiment. It is reasonable to surmise that the 2^-S wave seen in our data is a "leak through" from an A_3 which decays primarily into $f^0\pi^+$.

We now turn our attention to the 2^-P $(\bar{K}^{*0}(892)K^+)$ wave. The intensity shows a sharp peak in the 1.8—1.9 GeV/c^2 mass bin and the phase differences (Fig. 22) a sharp drop at the same mass. Because of the ambiguity in phase about $\pm180°$, we have chosen the phase value that minimizes the phase difference between two adjacent intervals. The other choice would result in phase changes of $\sim200°$ over a mass difference of 100 MeV. Such a change is highly unlikely. The violent phase behavior may be due to threshold effects or interference with the background. There are five interference events between 2^-S $(f^0\pi^\pi)$ and 2^-P in the 1.7—1.8 GeV/c^2 mass interval, for example. Certainly no possibility can be ruled out on the present evidence. It is, however, interesting to note that in the same analysis which first claimed evidence for a resonant A_3, there is another 2^- peak in the 2^-D $(f^0\pi^+)$ wave at 1.85 GeV/c^2.[19]

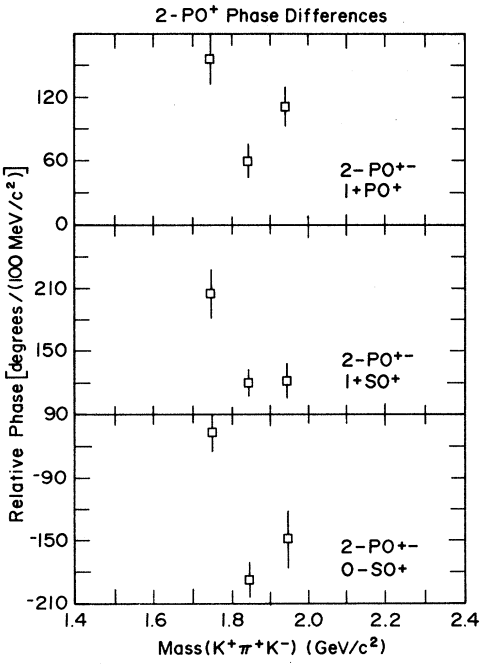

FIG. 22. The 2^-P phase differences with respect to the 0^-S, 1^+S, and 1^+P waves.

The final contribution to the 2^- state comes from the S-wave $\bar{K}^{*0}(1424)K^+$ system. The total number of events is small and the intensity featureless. There are modest increases in the phase differences, but no indications of an underlying resonance. As such, a Deck-type process may well be responsible for production. The cross section was determined to be 0.9 ± 0.2 μb.

CONCLUSIONS

The results we have presented illustrate above all the similarity between inelastic pion diffraction into $\pi\pi\pi$ and into $K\bar{K}\pi$. In both cases isobar formation gives a good description of the final state. Only low values of the relative angular momentum contribute, with S waves the predominant production mode. The Deck effect is seen in both reactions, particularly in the 1^+S wave. We, however, find no conclusive evidence for any resonance decaying into $K^+\pi^+K^-$.

Some of the most interesting aspects of the data are the mass enhancements that are seen both in this experiment and in three-pion reactions. We confirm the existence of a 0^-S mass peak in the 1.7—1.8 GeV/c^2 mass region, although none of the phase shifts show the 90° advance characteristic of a resonance. The 2^-S $(f^0\pi^+)$ wave shows no definable peak, but we have shown that the cross section, 1.3 ± 0.1 μb, is consistent with the interpretation that this state represents A_3 production in which the f^0 decays into K^+K^-. Again the phase shifts do not rise by 90°, but we believe that this is due to the mass range (300 MeV) in which the wave appears in our data. This in turn is a result of the limited statistics of this survey. The phase differences do, however, show the same increase over the same mass region as those seen in the three-pion data. There also exists a pronounced peak in the 2^-P wave between 1.8 and 1.9 GeV/c^2 which falls in the same area as a 2^-D $(f^0\pi^+)$ enhancement seen by the ACCMOR collaboration.[19] The phase shifts show a

sharp drop leaving any interpretation tenuous at best. Our results for the 1^+S wave tend to cast doubts on the claims of a high-mass (~ 1.3 GeV/c^2) A_1.[5] The 1^+S wave can be described well by pure Deck production, without the need of an A_1 decaying into $\bar{K}^{*0}(892)K^+$. Either the A_1 has a smaller mass, or it has a very small coupling to $\bar{K}^{*0}K^+$ in the momentum transfer interval examined.

Obviously differences do exist between $\pi\pi\pi$ and $K\bar{K}\pi$ diffraction. The κ is much more important in the latter state than the ϵ is in the three-pion case. This is in all likelihood due to the differences in threshold for the two reactions which are set by the onset of $\bar{K}^{*0}K^+$ and $\rho\pi$ production, respectively. The former occurs at 1.4 GeV/c^2 and the latter around 0.95 GeV/c^2. Since both κ and ϵ have masses of order 1.3 GeV/c^2, it is apparent that the κ should be produced more copiously. Another difference which is more dynamically related concerns the slopes of the differential cross sections which fall off more slowly in the $K\bar{K}\pi$ final state. In sum, though, it is our opinion that both reactions proceed by the same mechanism and produce similar results in spite of the differences in final states.

ACKNOWLEDGMENTS

This work was supported by U.S. Department of Energy. One of us (I.D.L.) would like to thank F. J. Loeffler for helpful discussions.

---

*Present address: Gulf Research Center, Pittsburgh, PA.

[1]G. Otter *et al.*, Nucl. Phys. B96, 365 (1975).
[2]G. Ascoli *et al.*, Phys. Rev. D 7, 669 (1973).
[3]G. Thompson *et al.*, Nucl. Phys. B69, 381 (1974).
[4]G. Thompson, J. A. Gaidos, R. L. McIlwain, and R. B. Willmann, Phys. Rev. D 9, 560 (1974).
[5]C. Daum *et al.* (ACCMOR Collaboration), Nucl. Phys. B182, 269 (1981).
[6]R. J. Cashmore, in *Experimental Meson Spectroscopy—1980,* proceedings of the Sixth International Conference, Brookhaven, edited by S. U. Chung and S. J. Lindenbaum (AIP, New York, 1981).
[7]J. L. Basdevant and Edmund L. Gerger, Phys. Rev. D 16, 657 (1977).
[8]J. Ballam and R. D. Watt, Ann. Rev. Nucl. Sci. 27, 75 (1977).
[9]*Landolt-Börnstein, New Series: Elastic and Charge Exchange Scattering of Elementary Particles,* I/7 (Springer, New York, 1973).
[10]I. D. Leedom, Ph.D. thesis, Purdue University, 1982 (unpublished).
[11]A. R. Moser, Ph.D. thesis, Purdue University, 1980 (unpublished).
[12]G. Thompson *et al.*, Phys. Rev. Lett. 32, 331 (1974).
[13]P. Bossetti *et al.*, Nucl. Phys. B101, 304 (1975).
[14]J. D. Hansen, G. T. Jones, G. Otter, and G. Rudolph, Nucl. Phys. B81, 403 (1974).
[15]G. Bellini *et al.*, Phys. Rev. Lett. 48, 1697 (1982).
[16]D. Z. Toet *et al.*, Nucl. Phys. B63, 248 (1973).
[17]E. P. Pietilainen and D. E. Lassila, Phys. Rev. D 16, 2803 (1977).
[18]P. Gavillet *et al.*, Phys. Lett. 76B, 517 (1978).
[19]C. Daum *et al.* (ACCMOR Collaboration), Phys. Lett. 89B, 285 (1980).